



OPEN ACCESS

Edited by:

Wen Zhou,
Case Western Reserve University,
United States

Reviewed by:

Ying Chen,
National Defense Medical Center,
Taiwan
Carl Friedrich Classen,
University Hospital Rostock, Germany

***Correspondence:**

Ignacio Camacho-Arroyo
camachoarroyo@gmail.com

Specialty section:

This article was submitted to
Cancer Endocrinology,
a section of the journal
Frontiers in Endocrinology

Received: 30 April 2021

Accepted: 11 January 2022

Published: 07 February 2022

Citation:

Del Moral-Morales A,
González-Orozco JC,
Hernández-Vega AM,
Hernández-Ortega K,
Peña-Gutiérrez KM
and Camacho-Arroyo I
(2022) EZH2 Mediates
Proliferation, Migration, and
Invasion Promoted by Estradiol
in Human Glioblastoma Cells.
Front. Endocrinol. 13:703733.
doi: 10.3389/fendo.2022.703733

EZH2 Mediates Proliferation, Migration, and Invasion Promoted by Estradiol in Human Glioblastoma Cells

Aylin Del Moral-Morales¹, Juan Carlos González-Orozco¹, Ana María Hernández-Vega¹, Karina Hernández-Ortega², Karla Mariana Peña-Gutiérrez² and Ignacio Camacho-Arroyo^{1*}

¹ Unidad de Investigación en Reproducción Humana, Instituto Nacional de Perinatología-Facultad de Química, Universidad Nacional Autónoma de México (UNAM), Ciudad de México, Mexico, ² Departamento de Biología, Facultad de Química, Universidad Nacional Autónoma de México (UNAM), Ciudad de México, Mexico

Glioblastomas (GBM) are the most frequent and aggressive brain tumors. 17 β -estradiol (E2) increases proliferation, migration, and invasion of human GBM cells; however underlying mechanisms are not fully understood. Zeste 2 Enhancer Homologous enzyme (EZH2) is a methyltransferase part of Polycomb 2 repressor complex (PRC2). In GBM, EZH2 is overexpressed and involved in the cell cycle, migration, and invasion processes. We studied the role of EZH2 in the pro-oncogenic actions of E2 in human GBM cells. EZH2 gene silencing and pharmacological inhibition of EZH2 blocked proliferation, migration, and invasion of GBM cells induced by E2. We identified *in silico* additional putative estrogen response elements (EREs) at the EZH2 promoter, but E2 did not modify EZH2 expression. *In silico* analysis also revealed that among human GBM samples, EZH2 expression was homogeneous; in contrast, the heterogeneous expression of estrogen receptors (ERs) allowed the classification of the samples into groups. Even in the GBM cluster with high expression of ERs and those of their target genes, the expression of PRC2 target genes did not change. Overall, our data suggest that in GBM cells, pro-oncogenic actions of E2 are mediated by EZH2, without changes in EZH2 expression and by mechanisms that appear to be unrelated to the transcriptional activity of ERs.

Keywords: glioblastoma, 17 β -estradiol, EZH2, estrogen receptor α , estrogen receptor β , PRC2

INTRODUCTION

Astrocytomas are primary tumors generated by the malignization of glial cells, glial progenitors, or transformed neural stem cells. According to their histopathological characteristics, the WHO classifies gliomas into four grades, grade IV or glioblastoma (GBM), as the most aggressive and frequent (1). GBMs are characterized by being highly invasive and fast-growing so that patients have a low life expectancy (12 to 16 months after diagnosis). Unfortunately, currently available therapies (surgery, chemotherapy, and radiation therapy) are not enough, as a 5-year survival rate is less than 5% (2, 3). Because GBMs are more frequent in males than in females, the role of sex hormones such as progesterone, 17 β -estradiol (E2), and testosterone in the incidence and progression of GBM has gained greater attention (4–6). Notably, E2 concentration is higher in GBM biopsies than in low-grade gliomas (7).

Moreover, E2 promotes the proliferation, migration, and invasion of cells derived from human GBM (4, 8). It has been recently shown that E2 is essential for epithelial to mesenchymal transition (EMT) of human GBM cells (9), which suggests that this hormone and its mechanisms of action are of great interest for the study of GBMs. Estrogens bind to specific intracellular and membrane receptors in cells. There are two estrogen-specific intracellular receptor subtypes, estrogen receptors α and β (ER α and ER β), which acts as ligand-activated transcription factors to regulate gene expression. Moreover, these receptors can associate with the plasma membrane, triggering intracellular signaling pathways (10, 11).

The Enhancer of Zeste Homolog 2 (EZH2) is an enzymatic part of the Polycomb Group (PcG), a set of transcriptional repressors that modify chromatin that controls the progression of the cell cycle and participates in the maintenance of cell differentiation (12). This group is represented by the Polycomb 1 and 2 repressor complexes (PRC1 and PRC2). PRC2 is the complex responsible for mono, di, and trimethylation of histone 3 in lysine 27 (H3K27me1/2/3) (13). The H3K27me3 tag is associated with gene promoters found in facultative heterochromatin and is read by PRC1, which binds to chromatin, preventing transcription (14). PRC2 has three essential core components: EZH2, a lysine-specific methyltransferase presenting a SET [Su(var) 3-9; E(z); Trithorax] catalytic domain; EED 1 (embryonic ectoderm development) containing WD40 [tryptophan–aspartate (WD) repeat] motifs that identify adjacent methylation marks in histones and anchor the complex to chromatin; and SUZ12, (Suppressor of Zeste 12) [Su(z)12 or its human homolog, JAZ1], a histone deacetylase

(15–17). EZH2 is known to be required to maintain cell identity and differentiation by repressing tissue-specific genes and proliferation inhibitors (12).

EZH2 is dysregulated in various types of cancer, including brain tumors (18–20). In GBMs, EZH2 functions as an oncogene. It is involved in multiple glioma cellular processes, including cell cycle, invasion, and glioma stem cell maintenance, which is thought to be responsible for drug resistance and tumor recurrence (13, 21). Besides, the expression of this gene is directly related to tumor malignancy, and its overexpression is associated with poor prognosis (19–21). Unfortunately, not much is known about the factors involved in regulating EZH2 gene expression and activity in GBM. However, in breast cancer, estrogen response elements (EREs) have been reported in promoter sequences of EZH2; moreover, E2 directly regulates the expression of EZH2 through its nuclear receptors (22). Also, in papillary thyroid carcinoma, E2 interacted with ER α and upregulated EZH2 (23). Given the above evidence, we speculate that in GBM, EZH2 expression could be regulated by E2 and that EZH2 participates in estrogenic actions on proliferation, migration, and invasion of GBM cells.

The present study characterized the EZH2 expression in human GBM-derived cell lines (U87, U251, and D54) and a set of glioma biopsies data from The Cancer Genome Atlas (TCGA). E2 induced no significant changes in EZH2 expression in the cell lines. However, silencing EZH2 or inhibiting its activity suppressed E2-induced proliferation, migration and invasion in GBM cells. Interestingly, *in silico* data analysis of GBM biopsies showed that ER α and ER β were heterogeneously expressed, so we grouped them into three hierarchical clusters. GBM cluster 3, with the highest expression of ERs and enriched in estrogen-regulated genes, showed no changes in PRC2/EZH2 target genes. Therefore, our results indicate that pro-oncogenic actions of E2 on GBM cells are mediated *via* EZH2 activity, without E2 modifying EZH2 expression. In GBM samples, the expression of ERs and their transcriptional actions were not directly related to those of EZH2, suggesting that E2 should modulate EZH2 by an extra-nuclear mechanism.

MATERIALS AND METHODS

Cell Culture and Treatments

Human GBM-derived cell lines U87, U251, and D54 (ATCC, WA, USA) were cultured in Dulbecco's Modified Eagle's medium (DMEM, *In vitro*, Mexico) high glucose supplemented with 10% fetal bovine serum (FBS), 1 mM pyruvate, 2 mM glutamine, and 0.1 mM non-essential amino acids. Cell cultures were maintained at 37°C in a humidified atmosphere with 5%. 24 h before treatments, the medium was changed by phenol red-free DMEM (*In vitro*, Mexico) supplemented with charcoal-stripped FBS (HyClone, USA). The following treatments were applied for 12 or 24 h: E2 (1 nM, 10 nM, 100 nM, and 1 μ M) and vehicle (V, 0.02% cyclodextrin). Cells were also treated with 5 μ M of GSK 343 (an S-adenosyl methionine, SAM-competitive inhibitor) or vehicle control (0.1% DMSO) to evaluate the effect of pharmacological inhibition of EZH2 (24). E2, Cyclodextrin

Abbreviation: BrdU, 5-Bromo-2'-deoxyuridine; CBs, Cajal bodies; E2, 17 β -estradiol; ECM, extracellular matrix; EED, 1 embryonic ectoderm development; EMT, epithelial to mesenchymal transition; EREs, estrogen response elements; ERs, estrogen receptors; ER α , estrogen receptors α ; ER β , estrogen receptors β ; EZH2, Zeste 2 Enhancer Homologous enzyme; GBM, glioblastoma; GO, gene ontology; GPER, G protein-coupled receptor; GSEA, gene set enrichment analysis; H3K27me1/2/3, histone 3 lysine 27 mono, di, and trimethylation; PcG, Polycomb Group; PRC1, Polycomb 1 repressor complex; PRC2, Polycomb repressor complexes; SET, Su(var) 3-9; E(z) Trithorax domain; SUZ12, Suppressor of Zeste 12; TCGA, The Cancer Genome Atlas; TSS, transcription start site; WD40, tryptophan–aspartate repeat motifs.

(CDX), GSK 343 and DMSO were purchased from Sigma Aldrich (USA).

RT-qPCR

According to the manufacturer's protocol, total RNA was extracted using TRIzol LS Reagent (Thermo Fisher Scientific, USA), and concentration was measured by spectrophotometry (NanoDrop 2000 Spectrophotometer, Thermo Fisher Scientific, USA). RNA integrity was verified by electrophoresis with a 1.5% agarose gel in Tris-Borate-ethylenediaminetetraacetic acid (EDTA) buffer using GreenSafe for visualization. Total RNA from Healthy Human Astrocytes (HA) was obtained from ScienCell Research Laboratories (USA). Total RNA (1 µg) was subjected to reverse transcription using the MMLV RT enzyme (Invitrogen, USA) and oligo-dT12-18 primers. Complementary DNA (cDNA) was amplified by RT-qPCR using the FastStart DNA Master SYBR Green I reagent kit for LightCycler 1.5 (Roche Diagnostics, Germany) following the manufacturer's protocol. Primers used were the following: EZH2 (25), (FW-5'-CCCTGACCTCTGCTTACTTGTGGA-3', RV-ACGTCAGATGGTCCAGCAATA-3'; 18S (FW-5'-AGTGAACTGC AATGGCTC-3', RV-5'-CTGACCGGGTTGGTTTTGAT-3'). Relative expression of the EZH2 gene was calculated considering the 18S mRNA gene as an endogenous reference. Relative expression levels were calculated by the $2^{-\Delta\Delta Ct}$ method (26, 27).

Western Blot

After treatments, cell pellets were lysed with RIPA buffer plus supplemented with protease inhibitors (1 mM EDTA, 2 µg/ml leupeptin, 2 µg/ml aprotinin, 1 mM PMSF). Total protein was obtained by centrifugation at 14,000 rpm, at 4°C for 5 min and quantified using Pierce Protein Assay reagent (Thermo Fisher Scientific, USA) in a NanoDrop 2000 Spectrophotometer (Thermo Scientific, USA). Thirty µg of total protein were separated on 10% SDS-polyacrylamide gel electrophoresis (PAGE) and transferred to a PVDF membrane at 25V in semi-dry conditions for 45 min. Membranes were blocked overnight with 5% bovine serum albumin (BSA, *In Vitro*, Mexico), at 4°C and then incubated for 24h with one of the following antibodies: EZH2 (5246S, Cell Signaling, USA), H3K27me3 (9733, Cell signaling, USA) and α -Tubulin (sc-398103, Santa Cruz Biotechnology, USA). Afterwards, membranes were incubated with horseradish peroxidase-conjugated secondary anti-rabbit (sc-2004, Santa Cruz Biotechnology, USA) at room temperature for 45 min. Finally, membranes were incubated with Super Signal West Femto Maximum Sensitivity Substrate (Thermo Scientific, USA) and then exposed to Kodak Biomax Light Film (Sigma-Aldrich, USA) for detecting immune complexes. Densitometric analysis of western blot bands was conducted using Image J 1.45S software (National Institutes of Health, USA). EZH2 and H3K27me3 contents were normalized to that of α -tubulin.

Immunofluorescence

U87, U251, and D54 cells were fixed with 4% paraformaldehyde solution (PFA) at room temperature for 20 min and washed with PBS. Then, cells were permeabilized and blocked (1% BSA, 0.2%

Triton X-100 in PBS) at room temperature for 30 min. Next, cells were incubated for 24 h with rabbit anti-EZH2 (5246S, Cell Signaling, USA) at 4°C and rinsed with PBST (PBS with 0.05% Tween). Later, cells were incubated with Goat anti-Rabbit IgG Alexa Fluor 647 (21246, Santa Cruz Biotechnology, USA) at room temperature for 60 min and rinsed with PBST. Nuclei were stained with 1 mg/mL Hoechst 33342 solution (Thermo Fisher Scientific, USA) at room temperature and again rinsed with PBST. Finally, cells were coverslipped using a fluorescence mounting medium (Polysciences Inc., USA) and visualized in an Olympus Bx43 microscope. For each condition, six arbitrary fields at 400X magnification were captured, and fluorescence density was measured with ImageJ software.

Bioinformatic Analysis of Response Elements

Gene sequence was obtained from the Human Genome Resources at NCBI (https://www.ncbi.nlm.nih.gov/genome/gdv/browser/?context=genome&acc=GCF_000001405.38). The promoter regions and transcription start site (TSS) were determined through the Ensembl database (28). Putative binding sites for ERs were searched with JASPAR (29), HOCOMOCO v.11 (30), and HOMER (v4.11) (31) platforms. Predicted binding sites by two or more databases with a score of 9 or greater and p-value < 0.05 were established as potential EREs.

siRNA Transfection

siRNA-mediated silencing of EZH2 was used to evaluate whether E2 effects on GBM proliferation, migration, and cell invasion are mediated through EZH2. Briefly, 2.5×10^5 U251 cells were seeded in 6-well plates in DMEM medium supplemented with 10% FBS and antibiotics. 24 h later, the medium was changed to DMEM phenol red-free medium without FBS and antibiotics. Then, using Lipofectamine RNAiMAX (Thermo Scientific, USA), cells were transfected with an EZH2 siRNA (10 nM, sc-35312, Santa Cruz Biotechnology, USA) or with a control siRNA (10 nM, sc-37007, Santa Cruz Biotechnology, USA) that does not induce any specific mRNA degradation. 24 h after siRNA transfection, the cell medium was refreshed, and 24 h later, cells were harvested for total protein extraction to determine EZH2 silencing efficiency through Western Blot.

Cell Proliferation Assays

Briefly, 2.5×10^5 U251 cells were transfected, as was described in the above section. 48 h after siRNA transfection, cells were treated with E2 (10 nM) or V (0.02% CDX) for 24 h. After treatment, cell proliferation was evaluated with the 5-Bromo-2'-deoxyuridine (BrdU) incorporation Kit I (Roche, USA) following the manufacturer's instructions. Additionally, the Hoechst staining (Thermo Scientific, USA) was used to counterstain the cell nuclei. BrdU and Hoechst fluorescence signals were analyzed under an Olympus Bx43F (Japan) microscope. The number of BrdU-positive cells was analyzed with the Image J software (NIH, USA). BrdU-positive cell percentage was calculated considering the total number of cell nuclei stained with Hoechst. In the case of pharmacological inhibition of EZH2, cells were treated with E2 (10 nM), CDX (0.02%) plus GSK 343 (5 µM), or vehicle (DMSO

0.01%) for 48 h. After treatments, cell proliferation was measured as described above.

Migration Assays

After siRNA transfection, cells were cultured for 24 h in phenol red-free DMEM medium supplemented with 10% hormone-free FBS. A scratch was made in the cell monolayer using a 200 μ l pipette tip, the removed cells were rinsed with PBS, and DMEM supplemented with hormone-free FBS was refreshed. One hour before adding treatments, cells were incubated with β -D-arabinofuranoside (Ara-C, 10 μ M, Sigma-Aldrich, USA) to inhibit cell proliferation; then, cells were treated with E2 (10 nM) or V (0.02% CDX) for 24 h. To assess migration under conditions of inhibition of EZH2 activity, cells were treated with E2 (10 nM), CDX (0.02%) plus GSK 343 (5 μ M), or vehicle (DMSO 0.01%) for 24 h. Images 100X of the wound area were captured at 0, and 24 h post-treatment with an Infinity 1-2 camera (Lumenera, Canada) attached to an Olympus CKX41 inverted microscope. Relative migration area distance (%) was calculated in four random fields of each experimental condition using the MRI Wound Healing Tool plugins of Image J software (National Institute of Health, USA).

Viability Assays

2.5×10^5 U251 cells were grown in DMEM medium supplemented with 10% FBS and antibiotics. 24 h later, the medium was changed to DMEM phenol red-free medium without FBS and antibiotics. Then, cells were transfected with an EZH2 siRNA (10153 nM, sc-35312, Santa Cruz Biotechnology, USA) or with a control siRNA (10 nM, sc-37007, Santa Cruz Biotechnology, USA). 48 h after siRNA transfection, cells were treated with E2 (10 nM) or V (0.02% CDX) for 24 h and then harvested with 1 mL PBS-EDTA (1 mM) and stained with trypan blue (0.4%). Viable cells were quantified with Countess II cell counter (Thermo Fisher Scientific, MA, USA).

Invasion Assays

The invasion potential of the cells was tested through Transwell assay using 10 μ m membrane thickness and 8 μ m pore size Transwell inserts (3422, Corning, Corning, USA) in 24-well plates. Extracellular matrix (ECM) gel from Engelbreth-Holm-Swarm murine sarcoma (2 mg/ml, matrigel E1270 Sigma-Aldrich, USA) was diluted with phenol red-free DMEM medium without supplement. It was placed in each well (50 μ l) and incubated at 37°C for 2 h. Next, on top of Transwell inserts, 2.5×10^5 cells were incubated in non-supplemented, phenol red-free DMEM medium (150 μ l) with Ara-C (10 μ M), and treatments (10 nM E2 or V). In the case of EZH2 inhibition, GSK 343 (5 μ M), or vehicle (DMSO 0.01%) were also used. The bottom part of the Transwell inserts was filled with 500 μ l of phenol red-free DMEM supplemented with 10% hormone-free FBS, acting as a chemoattractant. Then, the plate was incubated for 24 h at 37°C. Finally, after incubation for 24 h, cells from the upper surface of the membrane Transwells were washed, and cells that penetrated in matrigel (invading cells) were fixed with PFA 4% for 20 min and then stained with 0.1% crystal violet for 20 min. Images of invading cells were acquired at 100X magnification with an Infinity 1-2C camera (Lumenera,

Canada) connected to an inverted microscope (CKX41, Olympus, Japan). Cell number of four random fields per condition was determined with the Cell Counter plugin in the ImageJ software (National Institute of Health, USA).

Analysis of RNA-seq Data From TCGA and GTEx

Ribonucleic acid sequencing (RNA-seq) data of primary tumors from the low-grade gliomas (LGG, n=196) and GBM (n=139) projects of The Cancer Genome Atlas (TCGA-LGG and TCGA-GBM) were downloaded from the Genomic Data Commons portal of the National Cancer Institute (USA, <https://gdc.cancer.gov/>) using the “TCGAbiolinks” package for R v.3.5 (32). The transcriptome of 249 healthy cerebral cortex tissue samples was obtained from the GTEx database (<https://gtexportal.org/home/>). LGG includes grade I, II, and III gliomas. Data normalization and differential expression analysis were carried out with the DESeq2 v.1.22.2 (33) package. The graphs were built with the ggplot2 v3.2.1 (34) package.

Gene set enrichment analysis (GSEA) was carried out with the software of the same name, GSEA v.4.01 (35). All the gene sets used are available on the GSEA website <https://www.gsea-msigdb.org/gsea/index.jsp>. Gene ontology analysis was performed on the Enrichr platform (<https://maayanlab.cloud/Enrichr/>).

Statistical Analysis

Data from TCGA and GTEx were plotted and analyzed using R version 3.5.2. At least three biological replicates for each experiment approach were done. Experimental data were analyzed and plotted using the GraphPad Prism 5.0 software (GraphPad Software, CA, USA). Statistical analysis among groups was performed using a one-way ANOVA with a Tukey post-test. $p < 0.05$ was considered statistically significant.

RESULTS

EZH2 Is Expressed in Human GBM-Derived Cells

The expression of EZH2 was analyzed in three different cell lines derived from human GBM (U87, U251, and D54) and compared to those of normal human astrocytes (NHA) (**Figure 1A**). All three human GBM-derived cell lines (U87, U251, and D54) expressed EZH2 under basal conditions at the mRNA level. EZH2 expression in U251 and D54 was significantly higher than that of NHA. Significant differences were also found among cell lines, with U251 showing the highest expression level and U87 the lowest. The protein levels of EZH2 were also evaluated through Western blot in the GBM cell lines, and consistent with mRNA analysis, U251 cells showed the highest EZH2 content, while U87 cells had the lowest content (**Figure 1B**).

Subcellular localization of EZH2 was analyzed by immunofluorescence in U87, U251, and D54 cell lines. EZH2 was expressed in all cell lines, and it was mainly found in the nucleus, where it colocalizes with Hoechst dye, as shown in **Figure 1C**. As a negative control, immunofluorescence was

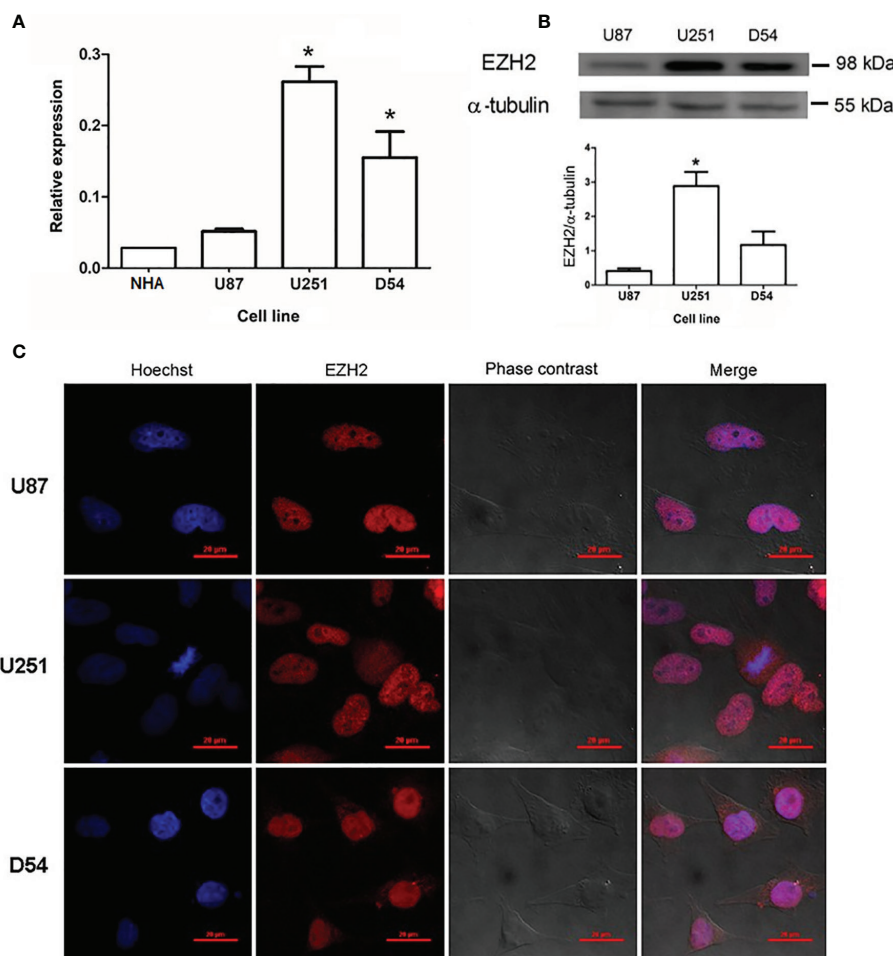


FIGURE 1 | Expression of EZH2 at mRNA and protein levels in human GBM-derived cells. **(A)** RT-qPCR quantified the amount of EZH2 mRNA (normalized to 18S ribosomal RNA using the comparative $2^{-\Delta\Delta Ct}$ method) in normal human astrocytes (NHA) and U87, U251, and D54 cell lines cultured under basal conditions. * $p < 0.05$ vs. U87 and NHA. Each bar represents the mean \pm S.E.M., $n = 3$. **(B)** EZH2 content was determined by Western blot in U87, U251, and D54 cell line, using α -tubulin as a loading control. Representative blot image and the corresponding densitometric analysis for EZH2 content in human GBM-derived cells. * $p < 0.05$ vs. U87 and D54. Bars represent the mean \pm S.E.M., $n = 3$. **(C)** Subcellular localization of EZH2 in GBM cell lines. Representative images of immunofluorescence showed that EZH2 is mainly found in the nuclei. Images were captured at 100X amplification. Red scale bars = 20 μ m.

performed without the monoclonal antibody against EZH2 (**Supplementary Figure 1**).

E2 Does Not Regulate EZH2 Expression in Human GBM

EREs have been reported in the EZH2 promoter, showing that E2 regulates the expression of the EZH2 gene in a couple of cancer cell types (22, 23). In addition to the EREs previously described (22), we found two potential EREs in the promoter region of the EZH2 gene by an *in silico* analysis (**Figure 2A**). The sequences of these putative binding sites and those early validated are shown in **Table 1**.

To evaluate the E2 regulation of EZH2 expression in GBM cells, U251, U87, and U251 cells were treated with E2 (10 nM) (4, 9) for 3, 6, 12, and 24 h. After treatment, EZH2 mRNA was quantified by RT-qPCR. Data showed that E2 significantly

induced EZH2 expression in the U87 line at 6 h of treatment. However, no significant changes were observed in U251 or D54 cells (**Figure 2B**). A curve of E2 concentrations was performed to rule out the possibility of a dose-dependent effect. The expression of EZH2 was evaluated through RT-qPCR at 12 and 24 h after treatment in U251 cells. However, no significant changes were detected in EZH2 gene expression (**Supplementary Figure 2**). E2 effect on EZH2 protein content was also analyzed by Western blot. E2 induced no significant changes in any cell lines at any evaluated times (**Figure 2C**). Therefore, it suggests that E2 does not regulate the expression of EZH2 in cell lines U87, U251, and D54.

EZH2 Silencing Inhibits E2-Induced Proliferation, Invasion, and Migration

In gliomas, EZH2 is involved in proliferation, invasion, and migration (19–21). E2 can also regulate these processes in GBM

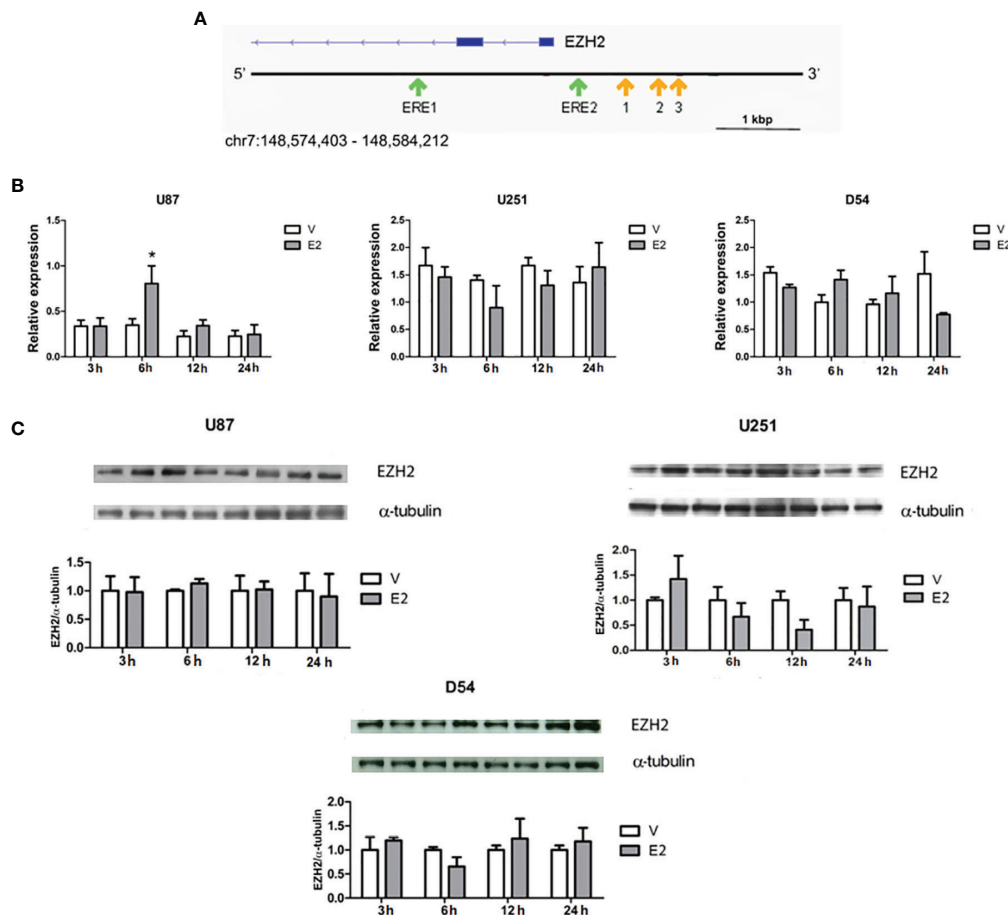


FIGURE 2 | E2 effect on EZH2 expression. **(A)** Schematic representation of the EZH2 gene is depicted in blue. The locations of EREs predicted by an *in silico* analysis are marked with green arrows. The analysis was performed on three different platforms (JASPAR, HOCOMOCO, and HOMER). A potential binding site was considered those predicted by two or more databases with a score value of 9 or higher and $p < 0.05$. Yellow arrows point to the binding sites previously described (22). Scale bar = 1 Kbp. **(B)** EZH2 expression was quantified by RT-qPCR after cell treatments with E2 (10 nM) or V (0.02% CDX) for 3, 6, 12, and 24 h. Relative expression of EZH2 mRNA was calculated by the $2^{-\Delta\Delta Ct}$ method using 18S ribosomal RNA as a reference gene. * $p < 0.001$ vs. V. Results are presented as mean \pm S.E.M. $n = 3$. **(C)** E2 effect on EZH2 content was also evaluated by Western blot. Densitometric analysis and corresponding representative images of EZH2 bands are shown. Each bar represents the mean \pm S.E.M, $n = 4$.

TABLE 1 | Sequences of EREs in EZH2 promoter.

Element	Position	Strand	Sequence
ERE1	-354 to -368	-	ATGTCTCCCGTCC
ERE2	+1599 to + 1586	-	TAATAACTTGCTTG
Sites reported by Bhan et al., 2016 (22).			
1	-846 to -859	-	GACCAGCCTGACC
2	-1238 to -1251	-	CGATCTCCTGACC
3	-1488 to -1501	-	AGGTAGCTTGACC

cells (4, 8, 9). Therefore, we decided to evaluate the impact of siRNA silencing of EZH2 on the pro-oncogenic actions E2-induced in the U251 cell line since it presented the highest levels of EZH2. First, the silencing efficiency of the siRNAs used was verified through Western blot. A decrease of close to 50% in EZH2 protein content was observed (Figure 3A). Also, we

measured cell viability by trypan blue exclusion assay in U251 cells treated with E2 (10 nM) and CDX after EZH2 inhibition by siRNA. We found no significant changes between treatments (Supplementary Table 1).

To determine whether the silencing of EZH modifies the proliferation induced by E2 in U251 cells, we performed a BrdU incorporation assay. E2 significantly stimulated the proliferation of U251 cells transfected with the control siRNA, compared to vehicle. However, in cells with silenced EZH2, no significant differences were observed between E2 or vehicle treatments (Figures 3B, C). A significant reduction in proliferation was observed in cells treated with E2 and EZH2 siRNA than those treated with E2 and control siRNA. These results show that EZH2 mediates that proliferation induced by E2 in U251 cells.

E2 also promotes migration and invasion of GBM-derived cell lines (4, 8, 9). To evaluate whether silencing of EZH2 also changes

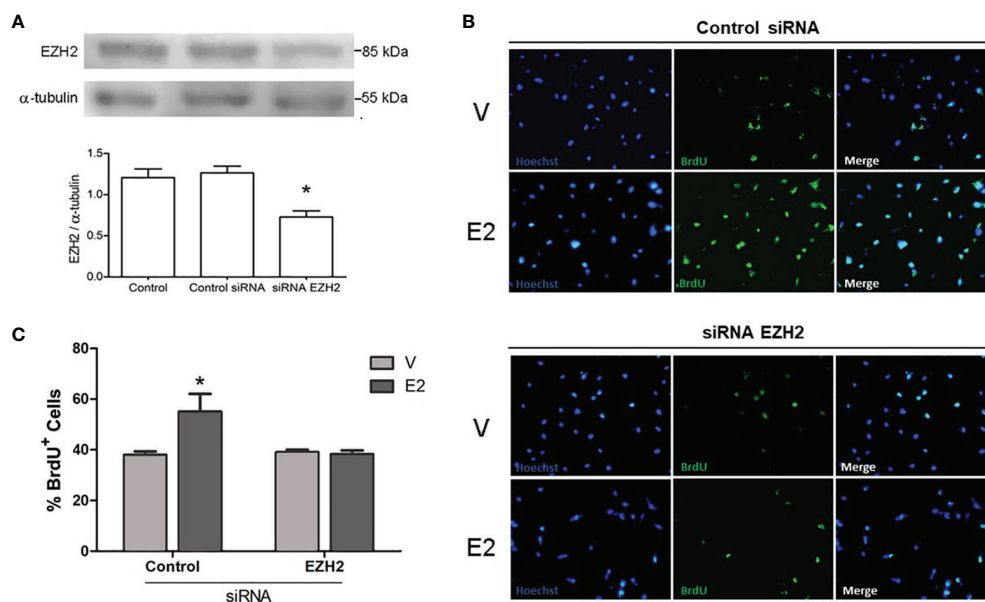


FIGURE 3 | Effect of EZH2 silencing on E2-induced proliferation. **(A)** Validation of EZH2 silencing. Representative Western blots of EZH2 content in U251 cells transfected with EZH2 siRNA or control siRNA interference (aleatory RNA sequence). Control: cells treated only with transfection reagent. Densitometric data are shown as mean \pm S.E.M. * $p < 0.05$. vs. the other groups. Analysis of proliferative capacity of U251 cells transfected with control siRNA or EZH2 siRNA and treated with E2 (10 nM) or V (0.02% CDX) for 48 h. **(B)** Representative images of BrdU incorporation in proliferating U251 cells, **(C)** and its corresponding quantification graphs showing the percentage of BrdU positive cells. Bars represent the mean \pm S.E.M. $n = 3$. * $p < 0.05$. vs. the other groups.

the migration induced by E2 in U251 cells, we carried out a wound-healing assay. Cells transfected with control siRNA and treated with E2 presented a higher migratory capacity than vehicle at 24 h after treatment. This increase was reversed when EZH2 was partially silenced (**Figures 4A, B**). A similar effect was observed when we evaluated invasiveness through a Transwell assay. E2 increased the number of invading cells (cells that penetrated in matrigel) transfected with control siRNA compared to the vehicle; however, in cells with silenced EZH2, we observed no significant differences in the cell number that penetrated the matrigel in E2 or vehicle conditions (**Figures 4C, D**). A significant diminution was found in invading cells treated with E2 and EZH2 siRNA compared with those treated with E2 and control siRNA. These observations show that EZH2 has an essential role in the promoting actions of E2 on proliferation, migration, and invasion in the U251 cell line.

Inhibition of EZH2 Activity Suppresses E2-Induced Proliferation, Invasion, and Migration

Since EZH2 silencing inhibits the pro-oncogenic actions E2-induced in the U251 cell line, we decided to evaluate whether inhibition of EZH2 activity also suppresses E2-induced proliferation, migration, and invasion; we used GSK343, which functions as a SAM-competitive EZH2 inhibitor. Treatment with GSK 343 (5 μ M) significantly reduced histone H3K27me3 in U251 cells, even when treated with E2 (**Supplementary Figure 3A**). Also, a substantial reduction in proliferation was

observed in cells treated with E2 and GSK 343 than those treated with E2 and DMSO (**Supplementary Figures 3B, C**). These results further support EZH2 activity mediates proliferation induced by E2 in U251 cells.

Next, we performed wound-healing and transwell invasion assays after GSK 343 and E2 treatments. Similarly, GSK 343 (5 μ M) suppressed the E2-induced increase in migratory (**Supplementary Figures 4A, B**) and invasive capacity (**Supplementary Figures 4C, D**) in U251 cells.

Differential Expression of EZH2 and ERs in GBM Biopsies

The above observations indicate that EZH2 is essential for E2 pro-oncogenic actions, and since E2 could alternatively modulate EZH2 activity *via* nongenomic signaling involving ERs (ER α and ER β) (36), we decided to explore whether there is a relationship between EZH2 and ERs expression in GBM. Therefore, transcriptomic data from low-grade glioma (LGG), GBM samples, and healthy human brain cortex samples obtained from the TCGA and GTEx platforms were analyzed.

Initially, we verified previous data indicating that EZH2 expression is higher in gliomas than in NT, increasing with tumor progression. EZH2 mRNA expression was higher in GBM than in LGG (**Supplementary Figure 5**), which supports the role of EZH2 in GBM progression (19–21). In an earlier report of our group, *in silico* analysis of a set of glioma samples revealed ER α expression was higher in NT than in gliomas. While, among gliomas, ER α mRNA was higher in GBM. Besides, a positive

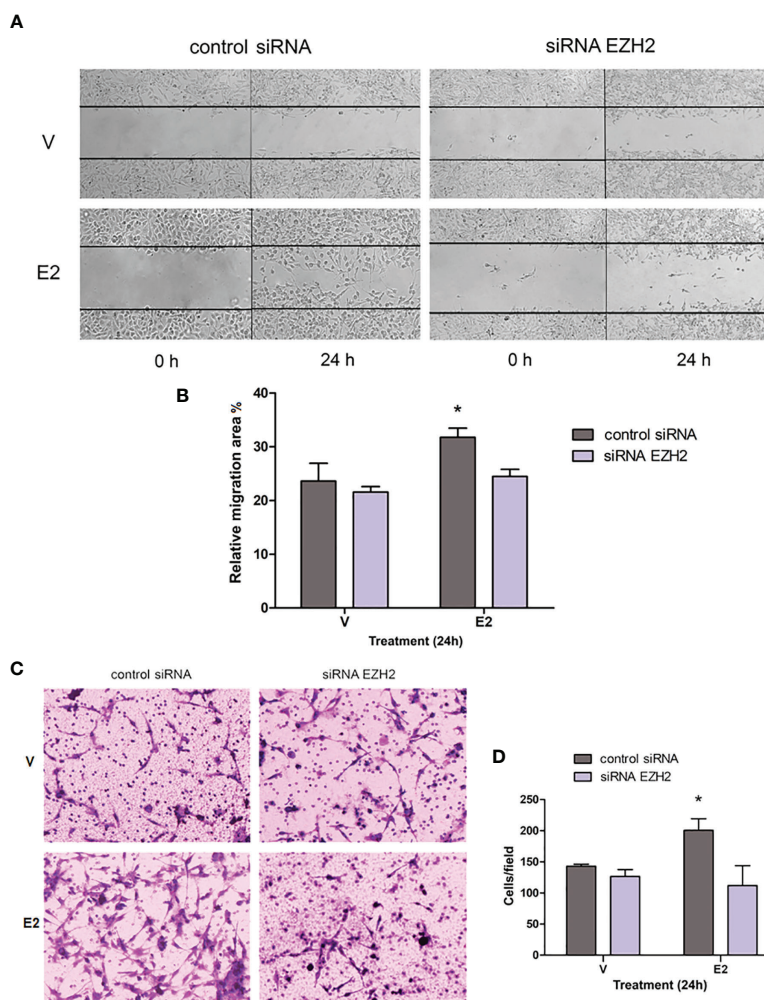


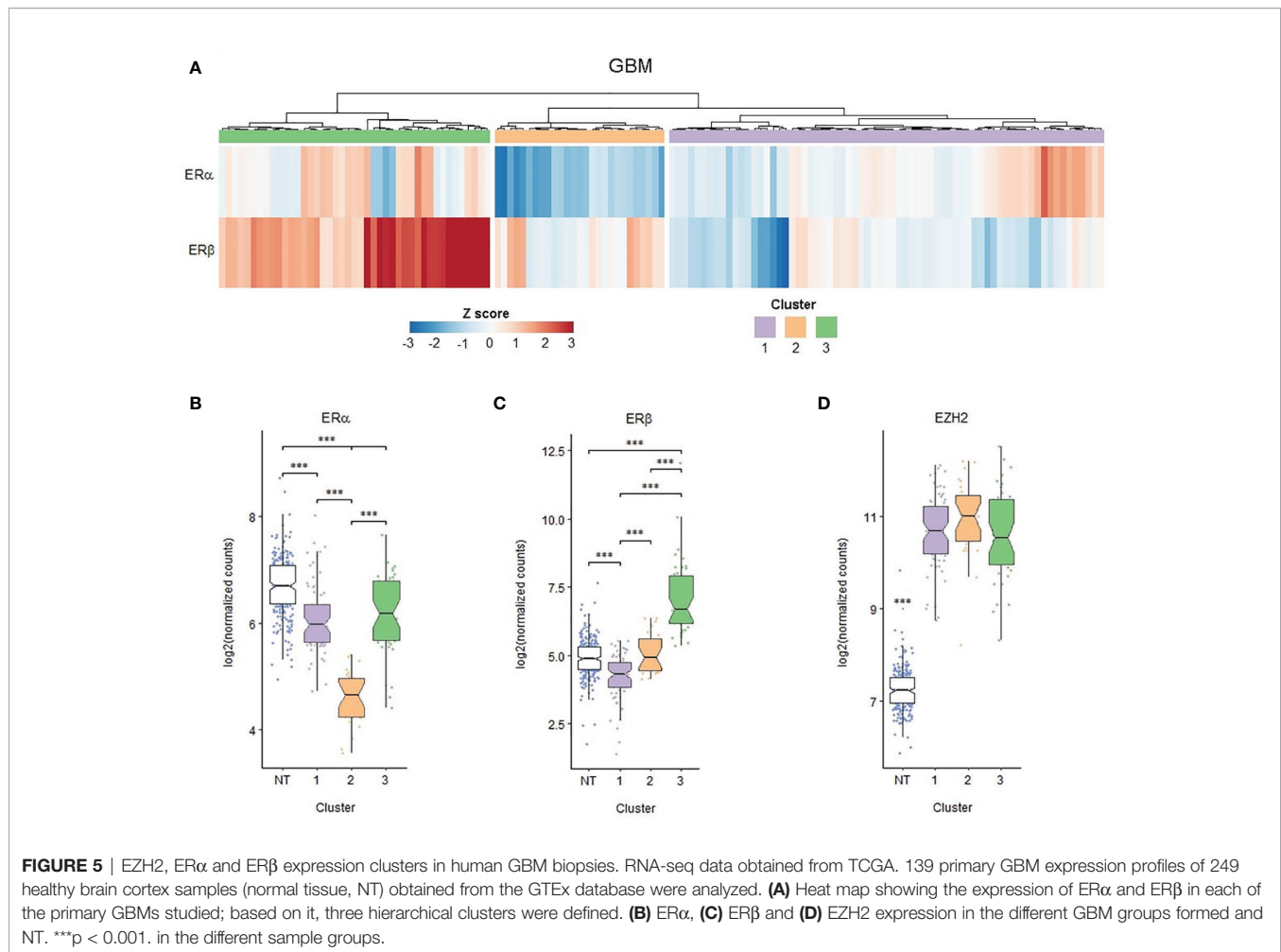
FIGURE 4 | Effect of EZH2 silencing on E2-induced migration and invasion. **(A)** Wound healing assays were performed in the U251 cell line transfected with control siRNA or EZH2 siRNA and treated with E2 (10 nM) or V (0.02% CDX). Representative images of the scratch area at 0 and 24 h. **(B)** Relative migration area (%) of U251 cells into wound area was measured 24 h after scratch formation. Graph data are shown as mean \pm S.E.M., $n = 3$. * $p < 0.05$, vs. the other groups. **(C)** Transwell assays were carried out in U251 cells treated as previously described. Representative photographs of the invading cells at the bottom of the transwells (cells that penetrated matrigel) stained with 0.1% cresyl violet after 24h of treatment **(D)** and the corresponding quantification. Results are expressed as the mean \pm S.E.M., $n = 3$. * $p < 0.05$, vs. the other groups.

correlation of ER- β expression with astrocytoma malignancy progress was evidenced (9). These observations indicated that the expression of ERs mRNAs was heterogeneous and did not coincide with that observed in EZH2 mRNA (**Supplementary Figure 5**), suggesting that ERs and EZH2 expressions are not related in gliomas progression.

To explore in detail the possibility of a relation between EZH2 and ERs expression, we focused our *in silico* analysis on GBM samples, which had the highest levels of EZH2. Since GBM samples presented a heterogeneous expression of ER α and ER β , they were stratified using the hierarchical grouping method. Our analysis showed that three clusters of GBM samples are distinguishable, as shown in **Figure 5A**. In group 1, ER α expression was high, and ER β expression was relatively low; group 2 had a slight expression of ER α , and medium expression

of ER β ; and group 3 presented high levels of both receptors, ER α and ER β (**Figures 5B, C**). The three GBM clusters had high EZH2 expression compared to NT; however, there were no significant differences (**Figure 5D**). In addition, we analyzed the sex composition of the different subgroups based on EZH2 and ERS expression, and we found that the composition of the GB subgroups is heterogeneous. There is no sexual dimorphism (**Supplementary Figures 6A–C**). Furthermore, the sex ratio is maintained in all three GB clusters, as indicated by a Chi-squared test (**Supplementary Figure 6D**).

We assessed whether the transcriptional activities of EZH2 and ERs are related to each other in GBM biopsy clusters with differential ERs expression levels. Differential gene expression data of GBM samples were used to carry out a Gene Set Enrichment Analysis (GSEA). In particular, we examined the



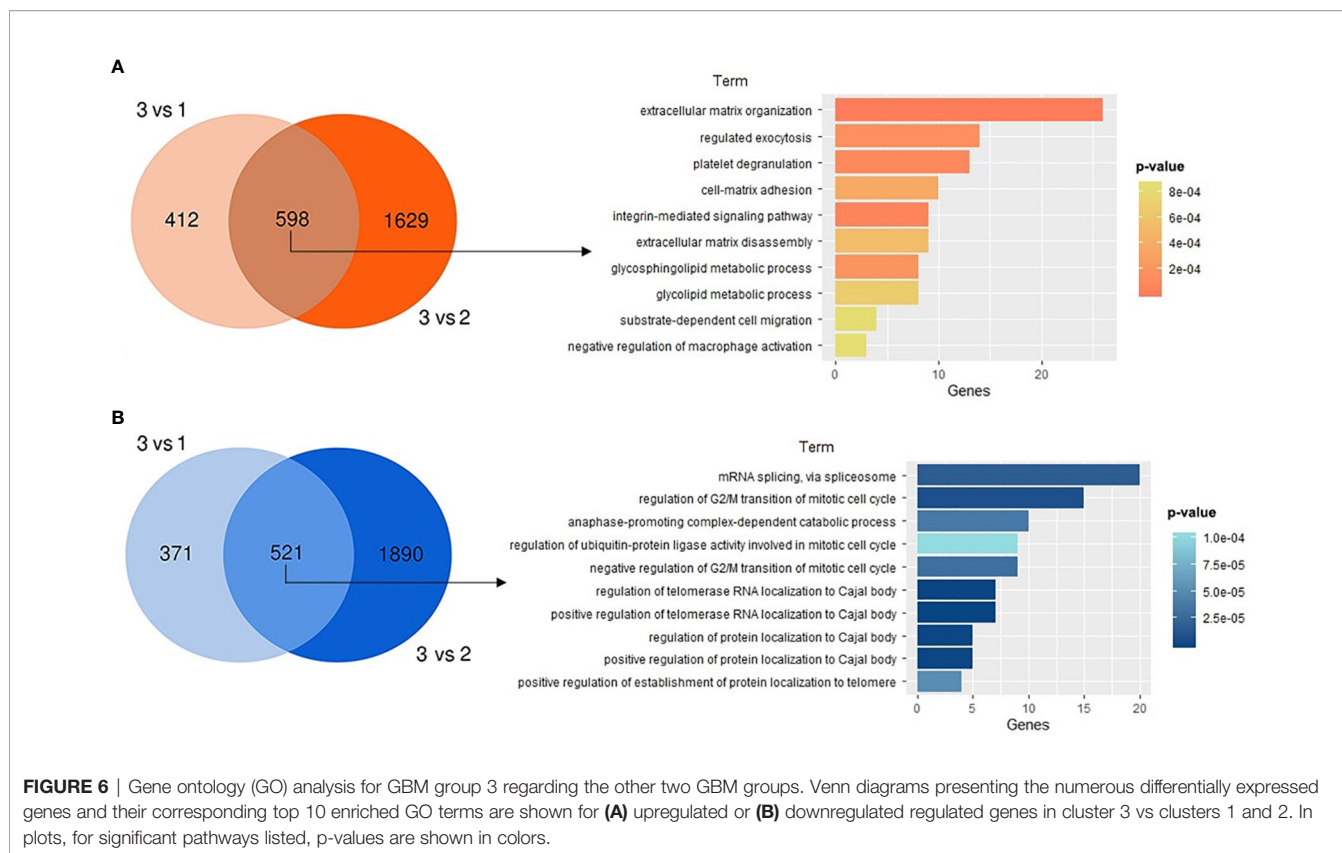
behavior of two expression gene sets: early estrogenic response and proven targets of the PRC2 complex, to which EZH2 belongs. It was observed that group 3 had a higher enrichment of early estrogen-responsive genes than groups 1 and 2. However, there were no significant differences between clusters in terms of downregulation or upregulation of the target genes of PRC2 (**Supplementary Figure 7**).

Finally, to expand the scope of the principal pathways modulated in GBM group 3 regarding the other two GBM groups (groups 1 and 2), differential expression analysis and the corresponding gene ontology (GO) annotation were performed. A core of 598 upregulated and 521 downregulated genes in group 3 versus the other two groups were analyzed to identify the corresponding top 10 corresponding enriched processes (**Figures 6A, B**). The processes mainly enriched in the upregulated genes in cluster 3 are those involved in extracellular matrix (ECM) organization and disassembly, regulated exocytosis, platelet degranulation, cell-matrix adhesion, and integrin-mediated integration signaling, among others. Enriched terms in downregulated processes mainly included mRNA splicing by the spliceosome, mitotic cell cycle regulation processes and, localization control of telomerase RNA and proteins to Cajal bodies (CBs).

DISCUSSION

In this work, we evaluated the participation of the methyltransferase EZH2 on E2 mediated pro-oncogenic effects in GBM cells. Moreover, using *in silico* transcriptomic data of GBM samples, we analyzed if ERs activities, as transcriptional regulators, could be related to those EZH2, as an approach to explore whether E2 mediates EZH2 activation through a genomic mechanism *via* its ERs.

First, to characterize EZH2 expression in cell lines derived from human GBMs, baseline expression of the EZH2 gene was evaluated in U87, U251, and D54 cell lines and compared to that of healthy human astrocytes. It was found that the three lines differentially expressed EZH2 at basal conditions and to a higher level than the control tissue. In this regard, several reports indicate that EZH2 is overexpressed in biopsies from GBM patients and that its expression is related to the tumor grade (19–21). The inter-tumoral heterogeneity in GBM cell lines can reflect differences in proliferation rate and cell contact inhibition, even when grown under the same conditions (37). Additionally, immunofluorescence results indicated that EZH2 was mainly located in the nucleus, suggesting that EZH2 protein was in a



functional state (by canonical mechanism) in the three GBM cell lines studied. In the case of U251 cells, we analyzed the content of H3K27me3, an indicator of EZH2 activity. Treatments with GSK 343, EZH2 inhibitor reduced histone H3K27trimethylation, suggesting that EZH2 present in U251 cells is active.

Considering that Bhan et al. previously reported the presence of EREs in the EZH2 promoter region (22) and that we found two others potential EREs through an *in silico* analysis, we decided to evaluate whether E2 (10 nM) treatments also regulate EZH2 expression in GBM cell lines. It is worth mentioning that the E2 (10 nM) concentration used is close to the E2 levels reported in GBMs biopsies (7). Moreover, it has been proven that E2 affects proliferation, migration, and invasion studies of GBMs cell lines (4, 8, 9). After E2 treatment, we observed no significant changes in EZH2 at either RNA or protein levels in GBM cells at any of the tested times. Even more, treatments with different concentrations of E2 (1 nM to 1 μ M) tested at 12 and 24 h confirmed that E2 did not induce the expression of EZH2 in U251 cells. These results contrast with those reported by Bhan et al. in breast cancer cell lines, whose EZH2 expression was induced by E2 (22). Although GBMs and breast cancer are estrogen-responsive tumors, they have different biological contexts in which the role of EZH2 and the mechanisms controlling its expression may be different, as has been suggested in neoplastic cells (14). EZH2 acts as an oncogene in various neoplasms such as breast cancer, prostate cancer, and GBMs (19, 38, 39). However, it can act as a tumor suppressor in

lymphomas and ovarian cancer (40–42). These data provide evidence of the complexity of the mechanisms regulating EZH2 expression and that its activity depends on the cellular context.

As mentioned earlier, E2 induces the proliferation, migration, and invasion of cell lines derived from human GBM (4, 8, 9); these processes are also promoted by EZH2 (13, 19, 21) activity. Therefore, we evaluated the impact of EZH2 silencing and EZH2 inhibition on these E2-induced processes. Since U251 presented the highest levels of EZH2, we decided to focus on it for subsequent analyses. E2 failed to induce proliferation, migration, and invasion when EZH2 was silenced or inhibited pharmacologically in U251 cells, suggesting that EZH2 mediates E2 effects on GBM cell lines. Although it has been previously reported that inhibition of EZH2 suppressed GBM growth, migration, and reversed EMT *in vitro* and *in vivo* (24, 43–45), this study is the first description demonstrating that EZH2 mediates E2 pro-oncogenic actions on GBM cells. Our results contribute to understanding the molecular mechanisms underlying GBM progression induced by E2 and EZH2 epigenetic mechanisms' participation.

The above observations indicated that EZH2 mediates E2-induced pro-oncogenic actions in GBM cells. Since E2 acts through ER α , and ER β , it raises the possibility of a relation between EZH2 and ERs in GBMs. Using transcriptomic data of LGG, GBM, and NT, we verified the previous evidence that EZH2 was overexpressed in glioma and correlated to the degree of tumor progression (19–21). An earlier report of our group

described a high ER β expression in glioma and low ER α expression compared to NT (9). At first glance, these data suggest that in gliomas, ERs and EZH2 expressions are not related. Nevertheless, we decided to evaluate this possibility in detail in GBM samples.

GBM is a highly heterogeneous tumor among gliomas at both the molecular and cellular levels (46). According to transcriptomic data, EZH2 mRNA was highly and homogeneously expressed in GBM biopsies, supporting its relevant role in GBM tumors. On the other hand, ER α and ER β expressions were highly heterogeneous. This characteristic allowed us to define three types of sample clusters and compare their mRNA expression profiles. In terms of the expression of ERs, especially ER α , and terms of the number of differentially expressed genes, cluster 3 (high ER α and ER β) exhibit more differences concerning cluster 2 (relatively low ER α and medium ER β) than cluster 1 (high ER α and very low ER β). It is worth mentioning that within each of these hierarchical subgroups, the sex ratio is maintained, so sex is not related to the levels of expression of the ERs according to which the three hierarchical groups were defined. When analyzing the expression of the set of early estrogenic response genes, these were enriched in GBM cluster 3 compared to the other two clusters. In contrast, just as EZH2 expression was similar among GBM clusters, the expression of the target genes of PRC2, the regulatory complex to which EZH2 belongs, was also homogeneous. These results show that high expression of ERs in GBM cluster 3 is associated with increased modulation of gene expression and reveal the leading role of ER α in such actions, including E2 target genes in GBM samples.

These results reveal a complex and heterogeneous mechanism underlying ERs actions in GBM. In this context, an essential role of ER α in GBM progression has been indicated by the observations of E2 induced cell growth of astrocytoma cell lines (4) and EMT activation in human GBM-derived cells through ER α (9). While, reports indicated that E2 increased proliferation from GBM (4), treatment with various ER β agonists reduced GBM cell proliferation (47). In other words, these data show that different ER subtypes modulate different actions in GBM. Also, we must consider that ERs expression levels may not always be proportional to their activity (48). In breast cancer cells, ER β significantly modifies a subset of ER α -dependent splicing (49). So, the cumulative sum of the particular actions of different ERs at a specific cellular context will define the overall cancer cell phenotype.

We performed a GO analysis to get an overall picture of the gene functions differentially modulated in GBM cluster 3 (high ER α and ER β) regarding the other GBM clusters with distinct ERs expression. Among biological/functional pathways mainly upregulated in GBM cluster 3, several are associated with pro-oncogenic actions promoted by E2 in cancer, even some of which are already described in GBM. For example, crosstalk between matrix components and ERs contributes to ECM remodeling and EMT in breast cancer (23). In GBM cluster 3, ECM organization/disassembly and cell-matrix adhesion terms were highly upregulated. Estrogens also regulate the expression

of genes that affect vesicle trafficking, including exocytosis, which affects the growth and metastasis of breast cancer cells (50, 51). Gene term of exocytosis regulated was overexpressed in GBM cluster 3. Increased expression of genes associated with platelet degranulation in GBM cluster 3 was also observed. Platelets play an essential role in cancer as they release permeability factors, degradative enzymes, and growth and angiogenic factors that assist tumor development progression and metastasis. In the ERs-positive subgroup of breast tumors, a high abundance of proteins related to platelet degranulation has been described (52). Integrin-mediated signaling pathway was also upregulated in cluster 3. It is known that ER β promotes migration through the Integrin β 1/MMP-9 pathway in normal colon epithelial cells (53). Importantly, outlining these upregulated gene terms, it emerges that most of them are compatible with the increase of migration and invasion processes induced by E2 in GBM cells (4, 8, 9).

Intriguing data concerning the downregulation of genes related to processing mRNA splicing, regulation of G2/M transition in cell cycle, and CBs associated process in GBM cluster 3 were found. It has been reported that ER β significantly affects ER α induced mRNA splicing in estrogen-responsive breast cancer cells (50), suggesting that ER β has considerably different and, in most cases, opposite biological effects compared to ER α . Regarding G2/M process modulation by E2, in human cervical cancer cells, non-classical membrane estrogen receptors G protein-coupled receptor (GPER) activation induced G2/M cell cycle arrest *via* EGFR/ERK1/2 signals (54). However, the participation of ER α and ER β in this sense is unknown. CBs mediate small nuclear and nucleolar ribonucleoproteins and telomerase assembly and modification. CBs are enriched in transcriptionally active and or with high splicing demands, such as cancer cells (55). Our analysis indicates significant deregulation of several pathways associated with CBs in GBM cluster 3 (high ER α and ER β).

The accumulated evidence of non-genomic signaling initiated by steroid receptors at membrane occurs in various cell types (10, 56). E2 can induce dimerization of ERs at the plasma membrane inducing fast signals by second messengers (e.g., cAMP, cGMP, Ca²⁺) and or activates kinase cascades that, in turn, may modulate nuclear transcription factors functions (57). In this regard, it has been reported that E2 regulates the activity of EZH2 through non-genomic signaling mediated by ER α and ER β leads, which leads to phosphorylation of EZH2 by AKT and MAPK pathways in benign and cancer prostate cells (36). Furthermore, post-translational modification of EZH2 can regulate its activity. For example, Akt phosphorylates EZH2 at serine 21 and suppresses its methyltransferase activity by impeding EZH2 binding to histone H3, which results in the derepression of silenced genes (58). Specifically, in GBM stem cells, AKT phosphorylates EZH2, and then it methylates STAT3 leading to enhanced STAT3 activity, which promotes GSC self-renewal and tumor malignancy (39). Recent work reported that overexpression of ER β isoform 5 (ER β 5) induced AKT phosphorylation and activation of STAT3, besides promoting migration of GBM cell lines (59). Persistent activation of STAT3

could be crucial for tumor progression and epithelium-mesenchyme transition (59, 60), a process also regulated by E2 in GBMs (9). Interestingly, in the set of evaluated biopsies, GBM samples have the highest expression of ER β , opening the possibility of assessing its participation in an extra-nuclear mechanism of E2 for mediating EZH2 activity in GBM cells.

In summary, in this work, we showed that in GBM cells, E2 induced proliferation, migration, and invasion through EZH2 without modulating its expression. Furthermore, in GBM samples, the expression levels of EZH2 are not related to those of the ERs, nor those of their target genes, suggesting that E2 induces EZH2 activation through a non-genomic mechanism that needs to be studied to clarify the outline of E2 pro-oncogenic activities in GBM.

DATA AVAILABILITY STATEMENT

The datasets analyzed in this study can be found in: <https://portal.gdc.cancer.gov/> and <https://gtexportal.org/home/>.

REFERENCES

- Louis DN, Perry A, Reifenberger G, von Deimling A, Figarella-Branger D, Cavenee WK, et al. The 2016 World Health Organization Classification of Tumors of the Central Nervous System: A Summary. *Acta Neuropathol* (2016) 131:803–20. doi: 10.1007/s00401-016-1545-1
- Hamza MA, Gilbert M. Targeted Therapy in Gliomas. *Curr Oncol Rep* (2014) 16:1–14. doi: 10.1007/s11912-014-0379-z
- Ostrom QT, Gittleman H, Truitt G, Boscia A, Kruchko C, Barnholtz-Sloan JS. CBTRUS Statistical Report: Primary Brain and Other Central Nervous System Tumors Diagnosed in the United States in 2011–2015. *Neuro Oncol* (2018) 20:iv1–iv86. doi: 10.1093/neuonc/noy131
- González-Arenas A, Hansberg-Pastor V, Hernández-Hernández OT, González-García TK, Henderson-Villalpando J, Lemus-Hernández D, et al. Estradiol Increases Cell Growth in Human Astrocytoma Cell Lines Through ER α Activation and its Interaction With SRC-1 and SRC-3 Coactivators. *Biochim Biophys Acta – Mol Cell Res* (2012) 1823:379–86. doi: 10.1016/j.bbamcr.2011.11.004
- Germán-Castelán L, Manjarrez-Marmolejo J, González-Arenas A, González-Morán MG, Camacho-Arroyo I. Progesterone Induces the Growth and Infiltration of Human Astrocytoma Cells Implanted in the Cerebral Cortex of the Rat. *BioMed Res Int* (2014) 2014:39317. doi: 10.1155/2014/393174
- Rodríguez-Lozano DC, Piña-Medina AG, Hansberg-Pastor V, Bello-Alvarez C, Camacho-Arroyo I. Testosterone Promotes Glioblastoma Cell Proliferation, Migration, and Invasion Through Androgen Receptor Activation. *Front Endocrinol (Lausanne)* (2019) 10:16. doi: 10.3389/fendo.2019.00016
- Dueñas Jiménez JM, Candanedo Arellano A, Santerre A, Orozco Suárez S, Sandoval Sánchez H, Feria Romero I, et al. Aromatase and Estrogen Receptor Alpha mRNA Expression as Prognostic Biomarkers in Patients With Astrocytomas. *J Neurooncol* (2014) 119:275–84. doi: 10.1007/s11060-014-1509-z
- Wan S, Jiang J, Zheng C, Wang N, Zhai X, Fei X, et al. Estrogen Nuclear Receptors Affect Cell Migration by Altering Sublocalization of AQP2 in Glioma Cell Lines. *Cell Death Discov* (2018) 4:49. doi: 10.1038/s41420-018-0113-y
- Hernández-Vega AM, Del Moral-Morales A, Zamora-Sánchez CJ, Piña-Medina AG, González Arenas A, Camacho-Arroyo I. Estradiol Induces

AUTHOR CONTRIBUTIONS

AM-M, JO, AH-V, KH-O, and KP-G carried out the experiments, data collection, and analysis. AM-M and IC-A conceived the experiments. AM-M and KH-O wrote the first draft of the manuscript, and IC-A contributed to the revision and editing of the manuscript. All authors have read and agreed to the published version of the manuscript.

FUNDING

This work was financially supported by Programa de Apoyo a Proyectos de Investigación e Innovación Tecnológica (PAPIIT), project number: IN217120. AD-M received a fellowship funding from CONACYT (CVU894530).

SUPPLEMENTARY MATERIAL

The Supplementary Material for this article can be found online at: <https://www.frontiersin.org/articles/10.3389/fendo.2022.703733/full#supplementary-material>

- Epithelial to Mesenchymal Transition of Human Glioblastoma Cells. *Cells* (2020) 9:1930. doi: 10.3390/cells9091930
- Arnal JF, Lenfant F, Metivier R, Flouriot G, Henrion D, Adlanmerini M, et al. Membrane and Nuclear Estrogen Receptor Alpha Actions: From Tissue Specificity to Medical Implications. *Physiol Rev* (2017) 97:1045–87. doi: 10.1152/physrev.00024.2016
- Fuentes N, Silveyra P. Estrogen Receptor Signaling Mechanisms. *Adv Protein Chem Struct Biol* (2019) 116:135–70. doi: 10.1016/bs.apcsb.2019.01.001
- Sauvageau M, Sauvageau G. Polycomb Group Proteins: Multi-Faceted Regulators of Somatic Stem Cells and Cancer. *Cell Stem Cell* (2010) 7:299–313. doi: 10.1016/j.stem.2010.08.002
- Yin Y, Qiu S, Peng Y. Functional Roles of Enhancer of Zeste Homolog 2 in Gliomas. *Gene* (2016) 576:189–94. doi: 10.1016/j.gene.2015.09.080
- Margueron R, Reinberg D. The Polycomb Complex PRC2 and its Mark in Life. *Nature* (2011) 469:343–9. doi: 10.1038/nature09784
- Gall Trošelj K, Novak Kujundzic R, Ugarkovic D. Polycomb Repressive Complex's Evolutionary Conserved Function: The Role of EZH2 Status and Cellular Background. *Clin Epigenet* (2016) 8:55. doi: 10.1186/s13148-016-0226-1
- Wiles ET, Selker EU. H3K27 Methylation: A Promiscuous Repressive Chromatin Mark. *Curr Opin Genet Dev* (2017) 43:31–7. doi: 10.1016/j.jgde.2016.11.001
- Li L, Zhang H, Zhang M, Zhao M, Feng L, Luo X, et al. Discovery and Molecular Basis of a Diverse Set of Polycomb Repressive Complex 2 Inhibitors Recognition by EED. *PloS One* (2017) 12:e0169855. doi: 10.1371/journal.pone.0169855
- Bachmann IM, Halvorsen OJ, Collett K, Stefansson IM, Straume O, Haukaas SA, et al. EZH2 Expression Is Associated With High Proliferation Rate and Aggressive Tumor Subgroups in Cutaneous Melanoma and Cancers of the Endometrium, Prostate, and Breast. *J Clin Oncol* (2006) 24:268–73. doi: 10.1200/JCO.2005.01.5180
- Zhang J, Chen L, Han L, Shi Z, Zhang J, Pu P, et al. EZH2 Is a Negative Prognostic Factor and Exhibits Pro-Oncogenic Activity in Glioblastoma. *Cancer Lett* (2015) 356:929–36. doi: 10.1016/j.canlet.2014.11.003
- Chen Yn, Hou Sq, Jiang R, Sun Jl, Cheng Cd, Qian Zr. EZH2 is a Potential Prognostic Predictor of Glioma. *J Cell Mol Med* (2021) 25:925–36. doi: 10.1111/jcmm.16149
- Chien YC, Chen JN, Chen YH, Chou RH, Lee HC, Yu YL. Epigenetic Silencing of Mir-9 Promotes Migration and Invasion by Ezh2 in Glioblastoma Cells. *Cancers (Basel)* (2020) 12:1–17. doi: 10.3390/cancers12071781

22. Bhan A, Hussain I, Ansari KI, Bobzean SAM, Perrotti LI, Mandal SS. Histone Methyltransferase EZH2 Is Transcriptionally Induced by Estradiol as Well as Estrogenic Endocrine Disruptors Bisphenol-a and Diethylstilbestrol. *J Mol Biol* (2014) 426:3426–41. doi: 10.1016/j.jmb.2014.07.025
23. Piperigkou Z, Karamanos NK. Estrogen Receptor-Mediated Targeting of the Extracellular Matrix Network in Cancer. *Semin Cancer Biol* (2020) 62:116–24. doi: 10.1016/j.semcancer.2019.07.006
24. Yu T, Wang Y, Hu Q, Wu WN, Wu Y, Wei W, et al. The EZH2 Inhibitor GSK343 Suppresses Cancer Stem-Like Phenotypes and Reverses Mesenchymal Transition in Glioma Cells. *Oncotarget* (2017) 8:98348–59. doi: 10.18632/oncotarget.21311
25. Fujii S, Ito K, Ito Y, Ochiai A. Enhancer of Zeste Homologue 2 (EZH2) Down-Regulates RUNX3 by Increasing Histone H3 Methylation. *J Biol Chem* (2008) 283:17324–32. doi: 10.1074/jbc.M800224200
26. Pfaffl MW. A New Mathematical Model for Relative Quantification in Real-Time RT-PCR. *Nucleic Acids Res* (2001) 29:e45. doi: 10.1093/nar/29.9.e45
27. Schmittgen TD, Livak KJ. Analyzing Real-Time PCR Data by the Comparative CT Method. *Nat Protoc* (2008) 3:1101–8. doi: 10.1038/nprot.2008.73
28. Zerbino DR, Achuthan P, Akanni W, Amode MR, Barrell D, Bhai J, et al. Ensembl 2018. *Nucleic Acids Res* (2018) 46:D754–61. doi: 10.1093/nar/gkx1098
29. Khan A, Fornes O, Stigliani A, Gheorghe M, Castro-Mondragon JA, van der Lee R, et al. JASPAR 2018: Update of the Open-Access Database of Transcription Factor Binding Profiles and Its Web Framework. *Nucleic Acids Res* (2018) 46:D260–6. doi: 10.1093/nar/gkx1126
30. Kulakovskiy IV, Vorontsov IE, Yevshin IS, Sharipov RN, Fedorova AD, Rumynskiy EI, et al. HOCOMOCO: Towards a Complete Collection of Transcription Factor Binding Models for Human and Mouse via Large-Scale ChIP-Seq Analysis. *Nucleic Acids Res* (2018) 46:D252–9. doi: 10.1093/nar/gkx1106
31. Duttke HS, Chang MW, Heinz S, Benner C. Identification and Dynamic Quantification of Regulatory Elements Using Total RNA. *Genome Res* (2019) 29:1836–846. doi: 10.1101/gr.253492.119
32. Colaprico A, Silva TC, Olsen C, Garofano L, Cava C, Garolini D, et al. TCGAAbiolinks: An R/Bioconductor Package for Integrative Analysis of TCGA Data. *Nucleic Acids Res* (2016) 44:e71. doi: 10.1093/nar/gkv1507
33. Love MI, Huber W, Anders S. Moderated Estimation of Fold Change and Dispersion for RNA-Seq Data With DESeq2. *Genome Biol* (2014) 15:550. doi: 10.1186/s13059-014-0550-8
34. Wickham H. *Ggplot2 - Elegant Graphics for Data Analysis*. 2nd ed. New York: Springer International Publishing (2016).
35. Subramanian A, Tamayo P, Mootha VK, Mukherjee S, Ebert BL, Gillette MA, et al. Gene Set Enrichment Analysis: A Knowledge-Based Approach for Interpreting Genome-Wide Expression Profiles. *Proc Natl Acad Sci USA* (2005) 102:15545–50. doi: 10.1073/pnas.0506580102
36. Majumdar S, Rinaldi JC, Malhotra NR, Xie L, Hu DP, Gauntner TD, et al. Differential Actions of Estrogen Receptor α and β via Nongenomic Signaling in Human Prostate Stem and Progenitor Cells. *Endocrinology* (2019) 160:2692–708. doi: 10.1210/en.2019-00177
37. Oraipoulou ME, Tzamali E, Tzedakis G, Vakis A, Papamatheakis J, Sakkalis V. *In Vitro/In Silico* Study on the Role of Doubling Time Heterogeneity Among Primary Glioblastoma Cell Lines. *BioMed Res Int* (2017) 2017:8569328. doi: 10.1155/2017/8569328
38. Sørensen KD, Ørntoft TF. Discovery of Prostate Cancer Biomarkers by Microarray Gene Expression Profiling. *Expert Rev Mol Diagn* (2010) 10:49–64. doi: 10.1586/erm.09.74
39. Kim E, Kim M, Woo DH, Shin Y, Shin J, Chang N, et al. Phosphorylation of EZH2 Activates STAT3 Signaling via STAT3 Methylation and Promotes Tumorigenicity of Glioblastoma Stem-Like Cells. *Cancer Cell* (2013) 23:839–52. doi: 10.1016/j.ccr.2013.04.008
40. Lee SCW, Phipson B, Hyland CD, Leong HS, Allan RS, Lun A, et al. Polycomb Repressive Complex 2 (PRC2) Suppresses E μ -Myc Lymphoma. *Blood* (2013) 122:2654–63. doi: 10.1182/blood-2013-02-484055
41. Scelfo A, Piunti A, Pasini D. The Controversial Role of the Polycomb Group Proteins in Transcription and Cancer: How Much do We Not Understand Polycomb Proteins? *FEBS J* (2015) 282:1703–22. doi: 10.1111/febs.13112
42. Koppens M, Van Lohuizen M. Context-Dependent Actions of Polycomb Repressors in Cancer. *Oncogene* (2016) 35:1341–52. doi: 10.1038/onc.2015.195
43. Cheng T, Xu Y. Effects of Enhancer of Zeste Homolog 2 (EZH2) Expression on Brain Glioma Cell Proliferation and Tumorigenesis. *Med Sci Monit: Int Med J Exp Clin Res* (2018) 24:7249–55. doi: 10.12659/MSM.909814
44. Stazi G, Taglieri L, Nicolai A, Romanelli A, Fioravanti R, Morrone S, et al. Dissecting the Role of Novel EZH2 Inhibitors in Primary Glioblastoma Cell Cultures: Effects on Proliferation, Epithelial-Mesenchymal Transition, Migration, and on the Pro-Inflammatory Phenotype. *Clin Epigenet* (2019) 11:173. doi: 10.1186/s13148-019-0763-5
45. Mishra VS, Kumar N, Raza M, Sehrawat S. Amalgamation of PI3K and EZH2 Blockade Synergistically Regulates Invasion and Angiogenesis: Combination Therapy for Glioblastomamultiforme. *Oncotarget* (2020) 11:4754–69. doi: 10.18632/ONCOTARGET.27842
46. Verhaak RGW, Hoadley KA, Purdom E, Wang V, Qi Y, Wilkerson MD, et al. Integrated Genomic Analysis Identifies Clinically Relevant Subtypes of Glioblastoma Characterized by Abnormalities in PDGFRA, IDH1, EGFR, and NF1. *Cancer Cell* (2010) 17:98–110. doi: 10.1016/j.ccr.2009.12.020
47. Sareddy GR, Nair BC, Gonugunta VK, Zhang QG, Brenner A, Brann DW, et al. Therapeutic Significance of Estrogen Receptor β Agonists in Gliomas. *Mol Cancer Ther* (2012) 11:1174–82. doi: 10.1158/1535-7163.MCT-11-0960
48. Hua H, Zhang H, Kong Q, Jiang Y. Mechanisms for Estrogen Receptor Expression in Human Cancer. Medical and Health Sciences 1112 Oncology and Carcinogenesis 06 Biological Sciences 0604 Genetics. *Exp Hematol Oncol* (2018) 7:24. doi: 10.1186/s40164-018-0116-7
49. Dago DN, Scafoglio C, Rinaldi A, Memoli D, Giurato G, Nassa G, et al. Estrogen Receptor Beta Impacts Hormone-Induced Alternative mRNA Splicing in Breast Cancer Cells. *BMC Genomics* (2015) 16:367. doi: 10.1186/s12864-015-1541-1
50. Wright PK, May FE, Darby S, Saif R, Lennard TW, Westley BR. Estrogen Regulates Vesicle Trafficking Gene Expression in EFF-3, EFM-19 and MCF-7 Breast Cancer Cells. *Int J Clin Exp Pathol* (2009) 2:463–75.
51. Mughees M, Chugh H, Wajid S. Vesicular Trafficking-Related Proteins as the Potential Therapeutic Target for Breast Cancer. *Protoplasma* (2020) 257:345–52. doi: 10.1007/s00709-019-01462-3
52. Brunoro GVF, Carvalho PC, Barbosa VC, Pagnoncelli D, De Moura Gallo CV, Perales J, et al. Differential Proteomic Comparison of Breast Cancer Secretome Using a Quantitative Paired Analysis Workflow. *BMC Cancer* (2019) 19:365. doi: 10.1186/s12885-019-5547-y
53. Shi T, Zhao C, Li Z, Zhang Q, Jin X. Bisphenol a Exposure Promotes the Migration of NCM460 Cells via Estrogen Receptor-Mediated Integrin β 1/MMP-9 Pathway. *Environ Toxicol* (2016) 31:799–807. doi: 10.1002/tox.22090
54. Zhang Q, Wu YZ, Zhang YM, Ji XH, Hao Q. Activation of G-Protein Coupled Estrogen Receptor Inhibits the Proliferation of Cervical Cancer Cells via Sustained Activation of ERK1/2. *Cell Biochem Funct* (2015) 33:134–42. doi: 10.1002/cbf.3097
55. Yao Y, Tan HW, Liang ZL, Wu GQ, Xu YM, Lau ATY. The Impact of Coilin Nonsynonymous Snp Variants E121k and V145i on Cell Growth and Cajal Body Formation: The First Characterization. *Genes (Basel)* (2020) 11:1–18. doi: 10.3390/genes11080895
56. Levin ER, Hammes SR. Nuclear Receptors Outside the Nucleus: Extracellular Signalling by Steroid Receptors. *Nat Rev Mol Cell Biol* (2016) 17:783–97. doi: 10.1038/nrm.2016.122
57. Levin ER. Membrane Estrogen Receptors Signal to Determine Transcription Factor Function. *Steroids* (2018) 132:1–4. doi: 10.1016/j.steroids.2017.10.014
58. Cha TL, Zhou BP, Xia W, Wu Y, Yang CC, Chen C, et al. Molecular Biology: Akt-Mediated Phosphorylation of EZH2 Suppresses Methylation of Lysine 27 in Histone H3. *Science* (2005) 316:310–0. doi: 10.1126/science.1118947
59. Liu J, Sareddy GR, Zhou M, Viswanadhappalli S, Li X, Lai Z, et al. Differential Effects of Estrogen Receptor B Isoforms on Glioblastoma Progression. *Cancer Res* (2018) 78:3176–89. doi: 10.1158/0008-5472.CAN-17-3470

60. Wendt MK, Balanis N, Carlin CR, Schiemann WP. STAT3 and Epithelial–Mesenchymal Transitions in Carcinomas. *JAK-STAT* (2014) 3:e28975. doi: 10.4161/jkst.28975

Conflict of Interest: The authors declare that the research was conducted in the absence of any commercial or financial relationships that could be construed as a potential conflict of interest.

Publisher's Note: All claims expressed in this article are solely those of the authors and do not necessarily represent those of their affiliated organizations, or those of the publisher, the editors and the reviewers. Any product that may be evaluated in

this article, or claim that may be made by its manufacturer, is not guaranteed or endorsed by the publisher.

Copyright © 2022 Del Moral-Morales, González-Orozco, Hernández-Vega, Hernández-Ortega, Peña-Gutiérrez and Camacho-Arroyo. This is an open-access article distributed under the terms of the Creative Commons Attribution License (CC BY). The use, distribution or reproduction in other forums is permitted, provided the original author(s) and the copyright owner(s) are credited and that the original publication in this journal is cited, in accordance with accepted academic practice. No use, distribution or reproduction is permitted which does not comply with these terms.